How to cite: *Angew. Chem. Int. Ed.* **2022,** *61,* e202203893
International Edition: doi.org/10.1002/anie.202203893
German Edition: doi.org/10.1002/ange.202203893

Physical Chemistry

Spectroscopic Fingerprints of Cavity Formation and Solute Insertion as a Measure of Hydration Entropic Loss and Enthalpic Gain

*Simone Pezzotti, Federico Sebastiani, Eliane P. van Dam, Sashary Ramos, Valeria Conti Nibali, Gerhard Schwaab, and Martina Havenith**

Abstract: Hydration free energies are dictated by a subtle balance of hydrophobic and hydrophilic interactions. We present here a spectroscopic approach, which gives direct access to the two main contributions: Using THz-spectroscopy to probe the frequency range of the intermolecular stretch (150–200 cm^{-1}) and the hindered rotations (450–600 cm^{-1}), the local contributions due to cavity formation and hydrophilic interactions can be traced back. We show that via THz calorimetry these fingerprints can be correlated 1:1 with the group specific solvation entropy and enthalpy. This allows to deduce separately the hydrophobic (i.e. cavity formation) and hydrophilic contributions to thermodynamics, as shown for hydrated alcohols as a case study. Accompanying molecular dynamics simulations quantitatively support our experimental results. In the future our approach will allow to dissect hydration contributions in inhomogeneous mixtures and under non-equilibrium conditions.

Hydrophobic hydration is important to understand and predict fundamental biological processes, such as protein folding and aggregation,[1–3] molecular recognition[4–6] and liquid-liquid phase separation,[7–9] as well as in many other fields, e.g. water-mediated catalysis[10–12] and electrocatalysis.[13–15] Going from small solutes all the way up to large biomolecules, a subtle balance between hydrophilic and hydrophobic interactions is what dictates hydration free energies.[16–24] Evaluating such balance requires a local mapping of hydrophilic and hydrophobic contributions, which remains a challenge for both theory and experiments.[18,19,25–29] From the experimental side, these contributions are notoriously difficult to probe and cannot be dissected by standard calorimetry approaches. Nevertheless, several attempts have been undertaken since the ability to characterize hydration thermodynamic properties would guarantee major economic advantages for e.g. drug discovery.[30] In the present work, we seek for a pathway to experimentally access both hydrophilic and hydrophobic contributions via THz-calorimentry[31] (i.e. via correlating THz vibrational fingerprints with entropy and enthalpy) and evaluate their synergy in dictating hydration free energies within a simple thermodynamic model.

A step-wise way to separate hydrophobic and hydrophilic contributions is to look at the hydration of a generic solute by adopting a thermodynamic cycle as illustrated in Figure 1.[32] It consists of a two-step process where 1) the water hydrogen bond (HB)-network is perturbed in order to create a cavity that can accommodate the solute; 2) the solute is inserted at the centre of the cavity, switching on attractive solute-water interactions. The total hydration energy is then given as the sum of the free energy of these two steps:

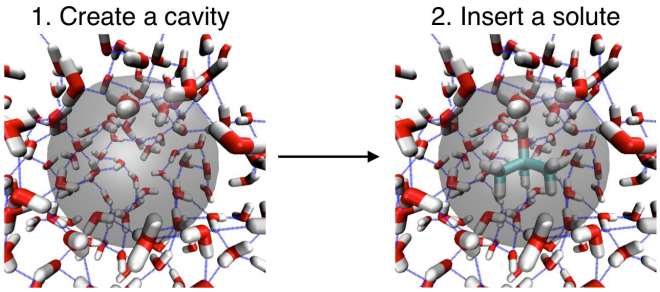

Figure 1. The hydration free energy of a generic solute can be modelled as a two-step process: 1) create a cavity in water where the solute can be accommodated, with associated free energy cost $\Delta\mu_{cavity}$; 2) insert a solute (tBuOH in the example) at the center of the cavity, with associated free energy gain $\Delta\mu_{bound}$. Hydration water molecules are illustrated with red oxygen and white hydrogen, H-Bonds are in blue. The alcohol (tBuOH) solute in step 2 is depicted with red oxygen, white hydrogen and cyan carbon atoms.

[*] S. Pezzotti, F. Sebastiani, E. P. van Dam, S. Ramos, V. Conti Nibali, G. Schwaab, M. Havenith
Department of Physical Chemistry II, Ruhr University Bochum
Bochum (Germany)
E-mail: martina.havenith@rub.de

F. Sebastiani
Current affiliation: Department of Chemistry "U. Schiff", University of Florence
I-50019 Sesto Fiorentino FI, (Italy)

V. Conti Nibali
Current affiliation: Dipartimento di Scienze Matematiche e Informatiche, Scienze Fisiche e Scienze della Terra (MIFT), Università di Messina
98166 Messina (Italy)

M. Havenith
Department of Physics, Technische Universität Dortmund
44227 Dortmund (Germany)

$$\Delta\mu_{hyd} = \Delta\mu_{cavity} + \Delta\mu_{bound} \quad (1)$$

The key aspect of this cycle is that $\Delta\mu_{bound}$ associated with step (2) is zero for a purely hydrophobic solute, which means that hydrophobic hydration is fully described by step (1), only. This latter step, which is associated to the free energy cost of cavity formation $\Delta\mu_{cavity}$, has been rationalized by the Lum–Chandler–Weeks (LCW) theory.[33] In a nutshell, hydrophobic solvation exhibits a pronounced length scale dependence and the LCW theory allows to analytically express the free energy cost to solvate both small and large hydrophobic solutes within a unified framework (given a-priori knowledge of equation of state, surface tension and radial distribution function of the pure liquid). For small solutes forming cavities of <1 nm radius (in the so-called volume-dominated regime), solvation requires a distortion of the water HB-Network, with associated entropic cost that scales with the cavity volume, while the solvation of larger solutes (in the so-called surface-dominated regime) induces formation of water dangling OH-groups, at an enthalpic cost that scales with the cavity surface area.

Building on our previous work,[27,31] we aim for a direct experimental characterization of the hydrophilic and hydrophobic contributions described by each of the two steps of Figure 1 and their interplay to determine the hydration free energy of molecules composed of both polar and apolar groups. Our study focuses on aqueous alcohol solutions as model systems, but the developed methodology can be generalized to more complex molecules and bio-interfaces, where the balance and distribution of polar and apolar groups are crucial parameters in determining hydration free energies and biological function.[16,18,26]

We have previously introduced THz absorption spectroscopy to characterize the water HB-network formed around hydrated solutes.[31,34] The THz spectrum of the solute and its hydration shell is obtained by subtracting the volume-scaled absorption spectrum of bulk water from the absorption spectrum of a solution containing the solute of interest.[27,31] Hydration-shell vibrational spectroscopies provide valuable information on the intermolecular interactions involving the solute and its hydration water molecules.[31,35–37] In our previous studies we focused on the HB intermolecular stretching region (100–300 cm^{-1}), i.e. the low frequency region showing the collective vibrations of the water HB-network, and we were able to identify two characteristic bands of the HB-network in the alcohol hydration layer. These were associated to HBs that spectroscopically, structurally and dynamically differ from the HBs formed in bulk liquid water. We observed these two characteristic bands for all alcohols from Methanol to Pentanol at varying concentration and temperature,[27,31] and similarly for clathrate hydrates[34] and for water interacting with extended hydrophobic surfaces.[38]

Specifically, water molecules in the closest proximity of the alcohol create a network of HBs wrapped around the whole solute (covering both hydrophilic OH and hydrophobic CH_2/CH_3 groups). This cavity forming HB-wrap provides a specific THz contribution centred at $\approx$164 cm^{-1}. A second population of HBs (HB-2bulk) connects hydration water to the bulk, and provides a specific THz contribution centred at $\approx$195 cm^{-1}, which is almost bulk like, with a narrower linewidth indicative of a reduced configurational space.[11,27] By THz-calorimetry we could quantitatively correlate the solvation entropy of all the alcohols to the amplitude of the two identified THz fingerprints.

While this provided an access to thermodynamic quantities from spectroscopy, we will show here that we are able to decompose hydration entropy, as obtained experimentally from THz-calorimetry, into the individual contributions from the CH_3, CH_2 and OH groups of alcohol molecules. This approach is suitable to evaluate how much the strong attractive interactions formed between the alcohol OH group and water alter hydration entropy with respect to the limit of only hydrophobic groups being solvated. While the hydrogen bond stretch region probes the strength of HBs, which is decreased for the HB-wrap, we show that the sterical restrictions for water molecules bound to the OH group (denoted hereafter bound waters) can be sensitively probed by the hindered reorientational motion of a single water molecule, i.e. the librational mode. Putting these results together makes it possible to experimentally map both steps of the thermodynamic cycle of Figure 1, hence revealing the interplay between hydrophilic and hydrophobic solvation mechanisms.

Building-blocks THz-calorimetry approach. We consider alcohols to be composed of three building blocks: CH_3, CH_2 and OH groups (Figure 2C). By using a large set of previously recorded[31] THz-calorimetry data for hydrated alcohols as database (MeOH, EtOH, PrOH, BuOH, tBuOH, PeOH), we derive here group-specific hydration entropies (ΔS_{hyd}) adopting a global fitting procedure detailed in section 4 of the Supporting Information. The idea is that ΔS_{hyd} of each alcohol can be rewritten as the sum of ΔS_{hyd} contributions from the building blocks composing it, i.e. $\Delta S_{hyd} = \sum \Delta S_{hyd}^{group}$. The approximation made here is that each group provides the same partial contribution (ΔS_{hyd}^{group}) for different alcohols. The hydration entropy values for all investigated alcohols have been previously obtained from THz-calorimetry,[27,31] and were found in excellent agreement with values from standard calorimetry. The working principles of THz-calorimetry are described in details in the Supporting Information.

The obtained ΔS_{hyd}^{group} values are reported in Figure 2A. CH_3 groups provide the largest contribution to the hydration entropy, followed by OH, while CH_2 groups contribute much less ($\approx$40 % of a CH_3). ΔS_{hyd}^{group} values obtained from classical MD simulations by means of a 3D-2PT model[27,39] (see Supporting Information, section 7 for details) are also reported for comparison (green curve). 3D-2PT allows to spatially resolve hydration entropy around hydrated alcohols. Group specific values are obtained by direct integration within the volume assigned to the hydration shell of each group. The validity of the building-blocks approximation used in the experimental procedure is testified by the good theory-experiments comparison. The differences in hydration entropy for polar (OH) and apolar (CH_2, CH_3) groups are attributed to i) a difference in the local water

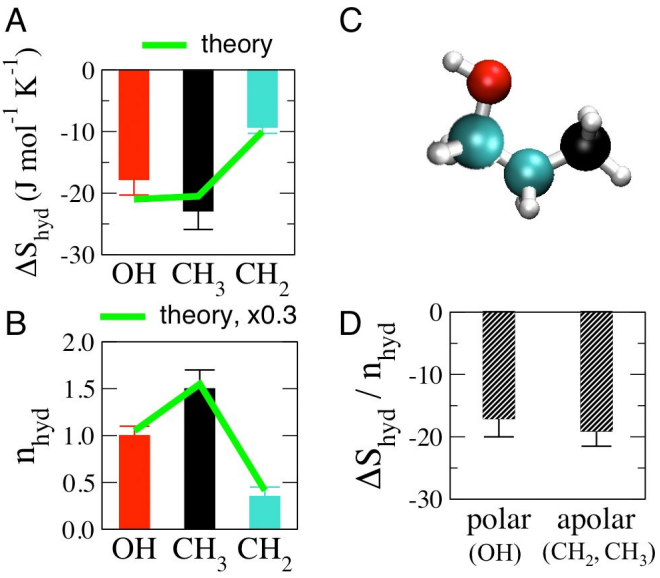

Figure 2. Group specific entropy contributions (at room temperature) to alcohol hydration from THz-calorimetry. A) Individual contributions of CH_3, CH_2 and OH groups to hydration entropy, ΔS_{hyd}. The green curve shows ΔS_{hyd} values predicted from classical MD simulations by means of a 3D-2PT approach. B) Effective hydration numbers (n_{hyd}) derived from THz experiments, compared to n_{hyd} values from MD simulations (green). The theoretical n_{hyd} values are arbitrarily scaled by 0.3 to compare with experiments, as they are obtained from direct counting of hydration water molecules while experimental values depend on spectroscopic activity. C) Illustration of the building blocks composing alcohols, i.e. CH_3 (black), OH (red), CH_2 (cyan). D) Experimental ΔS_{hyd} values divided by n_{hyd} and averaged separately over apolar (CH_2 and CH_3) and polar (only OH) groups.

structure around the groups or ii) a difference in the number of water molecules involved in the hydration of each group. Option (i) is unlikely to be the major contribution based on analysis of the structural, dynamical and vibrational properties of hydrated alcohols from ab initio and classical MD simulations. As shown in our previous work on hydrated tert-butanol,[27] the water molecules around apolar (CH_3) and polar (OH) groups all form on average three water-water HBs: 1.5 HB-wrap plus 1.5 HB-2bulk. They further have homogeneous water-water HB-dynamics within the inner part of the hydration layer. The difference is that bound water molecules interacting with the alcohol OH-group form an additional HB with the alcohol. In Figure 2D, we show experimentally-deduced partial hydration numbers (n_{hyd}) for each group and we compare them with theoretical values obtained from direct counting of the water molecules in the hydration shell of each group (the values are averages over tBuOH, BuOH and MeOH). The CH_3 groups, which provide the largest contribution to hydration entropy, also have the largest n_{hyd}, and the trend of n_{hyd} mirrors that observed for ΔS_{hyd}. If we divide ΔS_{hyd} by n_{hyd} and average over apolar (CH_2 and CH_3) and polar (only OH) groups separately, group-specific hydration entropy values per hydration water molecule for polar and apolar solvated moieties are obtained (Figure 2D, which show no differences). Interestingly, beyond the difference in the number of water molecules required to hydrate each group, we find that polar and apolar groups contribute equally to the hydration entropy of alcohols solutes. Thus, we propose that the entropic cost of alcohol hydration does not significantly depend on the specific HB interactions formed by the polar OH group with bound water molecules. The solute-bound water HBs, which are associated to step (2) of the thermodynamic cycle of Figure 1, mostly contribute as an enthalpic gain to alcohol hydration, due to the additional HB that bound water molecules form with the alcohol OH functional group. This is confirmed by adopting our group-specific THz-calorimetry approach to decompose alcohol hydration enthalpy (ΔH_{hyd}) into CH_2, CH_3 and OH contributions (see Supporting Information, Figure S3): we find that OH groups provide the dominant contribution (-7.7 ± 0.7 kJ mol^{-1} at room temperature) to ΔH_{hyd}.

These results have important implications for the thermodynamic cycle of Figure 1: the entropic cost of alcohol hydration is to a good approximation independent on step (2), i.e. independent on attractive alcohol-water interactions. In other words, the process of cavity formation, i.e step (1), dominates alcohol hydration entropy. This explains why the LCW theory has been highly successful in predicting alcohol hydration entropy[2] despite not directly accounting for the interactions formed by the hydrated solute with water.

THz fingerprint of bound water molecules. While the THz-fingerprints in the HB-stretching region probe cavity formation and associated entropic cost, we were lacking so far a direct THz-fingerprint for the second step of our thermodynamic cycle, i.e. for water molecules H-Bonded to the alcohols OH group. To fill this gap, we recorded THz-spectra of alcohol-water mixtures in the 100–600 cm^{-1} frequency range, significantly extending the frequency range with respect to previous measurements.[31] We hence move our attention from the HB-stretching region (100–300 cm^{-1}) to the onset of the librational band of water (300–600 cm^{-1}). In this frequency region we probe characteristic soft librations at lower frequencies (<400 cm^{-1}), and hard librations at higher frequencies (400–600 cm^{-1}), indicative of less or more hindered motions of the water molecules, respectively (alcohol specific motions are also active in this region, but not significant, as detailed in section 5 of the Supporting Information). In Figure 3A, we report the difference THz spectrum of hydrated tBuOH with respect to bulk water for different temperatures. We systematically observe an absorption decrease below 400 cm^{-1}, followed by an increase in the 400–600 cm^{-1} region. Similar trends are obtained for all the alcohols at various concentrations and temperatures (see Supporting Information and Figure S2 for details). Figure 3B displays the theoretical THz spectrum calculated from ab initio MD simulations by considering only the contribution of bound water molecules around a single tBuOH solute (including both the self and cross correlation terms, see Supporting Information and ref. [27]) for comparison.

Based on the theory-experiments comparison, we conclude that the absorption increase in the 450–600 cm^{-1} region is the direct spectroscopic signature of bound water

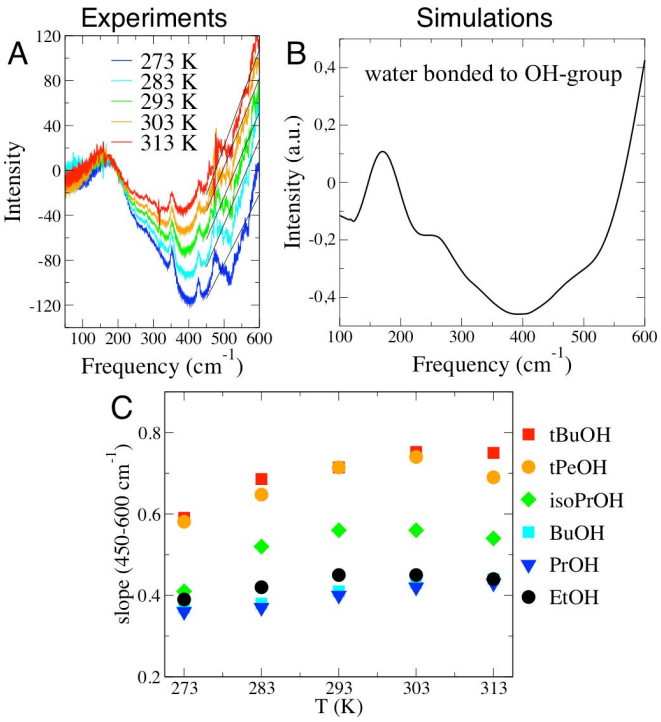

Figure 3. THz signature of the bound water population. A) Experimental hydration-shell resolved THz spectra of hydrated tBuOH at various temperatures, showing a characteristic intensity increase in the 400–600 cm^{-1} region. The black solid lines are linear fits of the THz intensity in the 450–600 cm^{-1} region, from which the slope plotted in panel C is obtained. B) Theoretical THz spectrum calculated from DFT-MD (same as in ref. [27]) considering only the contribution (both self and cross correlation terms) of bound water molecules hydrating the polar OH group of tBuOH. C) Slope of the THz-intensity in the 450–600 cm^{-1} region for various experimentally investigated alcohols as a function of temperature.

molecules. These water molecules are indeed found from classical MD to have more constrained orientational motions as compared to the other water molecules in the hydration layer or in the bulk, which is consistent with a blue shift in the librational mode. In particular, we computed orientational lifetimes of 4.4 ps for bound waters, 2.9 ps for the remaining water molecules in the hydration layer, and 1.9 ps for bulk water. This trend is well rationalized by the jump model of water reorientation:[40] Water orientational dynamics is expected to slow down in the hydration layer[41] due to an entropic excluded volume effect.[42] Moreover, an additional enthalpic effect contributes to the slow down for bound water molecules as they form a HB with the OH-group, further increasing the activation barrier for a jump. This is consistent with a population increase in the hard-librations and a loss in population of soft-librations, as observed experimentally. We want to mention that a similar absorption increase in the THz spectra at frequencies $>400\ cm^{-1}$ has been previously reported for hydration water molecules as a result of strong interactions with ions or with polar groups of biomolecules.[43–45] In order to quantify this effect, we take the slope of the absorption increase in the 450–600 cm^{-1} region and we compare it for different alcohols in Figure 3C. Remarkably, a similar slope is measured for EtOH, PrOH and BuOH, which are all primary alcohols (i.e. the C atom carrying the OH group is bonded to one C atom only). The slope is independent on the number of apolar CH_2 and CH_3 groups contained in the alcohol under investigation. This confirms our assignment of the band to the bound water population at the alcohol OH-group. Accordingly, the slope changes as soon as the environment of the OH groups is altered, i.e. when going from primary to secondary (iso-PrOH, for which the C atom carrying the OH group is bonded to two C atoms) and tertiary (tBuOH, tPeOH) alcohols. This is attributed to increased steric hindrance for the water molecules in the surrounding of the OH group, as confirmed by classical MD simulations that predict a slower orientational dynamics for bound waters around tBuOH as compared to BuOH (4.4 vs 3.8 ps). This result is expected due to the increase in volume excluded effect around the OH-group of a tertiary vs primary alcohol.[40,42] As a final confirmation of our assignment, we note that the two tertiary alcohols have a different number of apolar groups, but the same slope. Therefore, our results demonstrate that the 450–600 cm^{-1} librational region probes bound water molecules hydrating hydrophilic groups, which are associated to the second step of the thermodynamic cycle introduced in Figure 1. This additional fingerprint can be now used to map hydrophilic hydration free energies within the framework introduced in the present work.

In conclusion, we have developed a THz-calorimetry approach that enables to experimentally probe local contributions to hydration entropy and enthalpy and test existing theories of hydrophobic hydration. This approach quantitatively connects spectroscopic to thermodynamics quantities. Moreover, at variance with standard calorimetry, it can resolve local contributions to solvation entropy and enthalpy arising from hydration water populations as identified through their spectroscopic fingerprints. With this approach, we have shown experimentally that alcohol hydration is well described by a two-step thermodynamic cycle, where 1) a cavity is formed in the liquid, and 2) a solute is inserted at the center of the cavity, switching on attractive solute-water interactions. The free energy cost of cavity formation (i.e. the hydrophobic cost) can be quantified experimentally via THz-calorimetry by a characteristic HB-wrap mode at 164 cm^{-1}, in the HB-stretching region. The free energy gain from step (2) is dominated by the H-Bonds formed between the alcohol OH group and bound water molecules. The latter provide a THz fingerprint in the 450–600 cm^{-1} librational region. THz spectroscopy hence allows directly probing independently both hydrophobic and hydrophilic contributions to hydration free energies, as summarized in Figure 4. By using THz-calorimetry to relate spectroscopy to thermodynamics, we have shown that small alcohol hydration is a balance between entropic (hydrophobic) cost of cavity formation and enthalpic (hydrophilic) gain due to H-Bonds between the alcohol and bound waters. The entropic cost is almost independent on attractive solute-water interactions. Such behavior was previously predicted from theory for alkanes,[46] which do not strongly interact

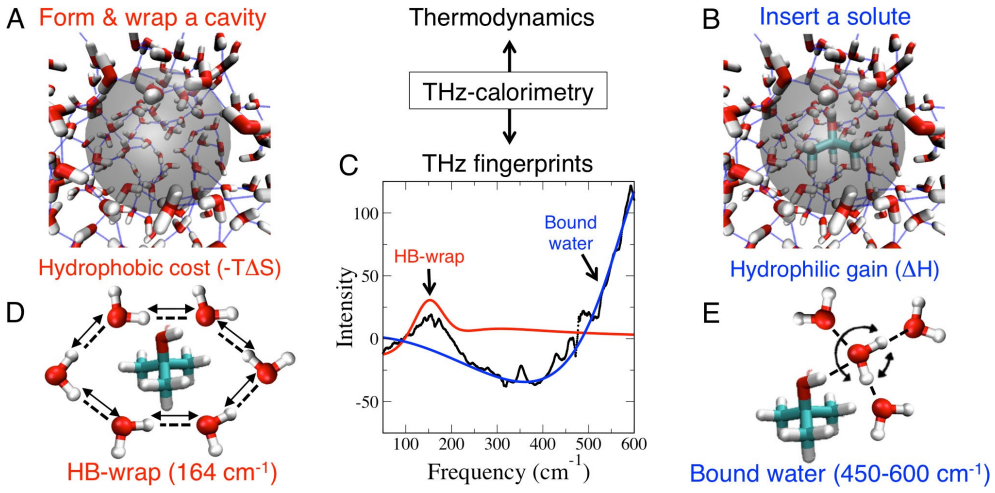

Figure 4. Small alcohol hydration free energy is the sum of A) an entropic cost of cavity formation, involving formation of a HB-wrap over the whole hydration layer, and B) an enthalpic gain due to the attractive interactions formed by the alcohol OH group with bound water molecules. C) THz-calorimetry quantifies both terms from THz translational (due to HB-stretching, red) and librational (blue) fingerprints of the hydration layer. In the example, the THz spectrum at room T is decomposed into the two terms for tBuOH. D) The 164 cm^{-1} THz fingerprint in the HB-stretching region probes the HB-wrap, while E) the librational band probes bound water molecules.

with water. We show here that the same conclusion holds true for solutes such as alcohols possessing a polar group that can H-Bond water. This is possible because alcohol-water interactions do not require significant restructuring of the water network in the hydration layer (i.e. of the HB-wrap) with respect to the empty cavity limit, as confirmed by analysing H-Bond connectivity and dynamics within the hydration layer from MD simulations (present study and ref. [27] for more details). We propose that solutes with the described properties can be classified as "wrappable", since alcohol-water interactions are well commensurate to the HB-wrap formed in the hydration layer. Our framework hence anticipates an effect of the topological and morphological aspects of the solute (being it a small molecule or an extended surface) on its hydration free energy and solubility. Such effects were observed in previous theoretical studies[16,26,47,48] of biological interfaces, and our approach offers a path for an experimental confirmation of these important findings. Furthermore, our results have important implications for applications of the LCW theory to rationalize solvation thermodynamics in general. Applications of the LCW theory (which neglects attractive solute-water interactions) rely on the implicit assumption that the cavity formation term dominates for "sufficiently hydrophobic" solutes. So far, this assumption could not be directly tested experimentally, and our approach makes it possible to do so, as we have shown here for small alcohols. As a perspective, recent theoretical studies proposed that more complex behaviors could arise when increasing the solute size: Hande et al.[49] proposed that the length-scale cross-over predicted by the LCW theory does not take place for large alcohols, while Coe et al.[50] showed that vapor bubbles formed at the interface between water and extended hydrophobic surfaces have a prominent effect on hydration free energies. These new findings call for further refinement of our theoretical understanding, and THz calorimetry will be a valuable tool to confirm and possibly improve these models.

In future studies, the THz fingerprints of wrap and bound hydration water populations can be also used to rationalize and quantify local thermodynamic contributions to more complex biomolecule hydration. It will allow to experimentally dissect the role that hydrophobic and hydrophilic interactions play in many biological processes, such as biomolecular recognition, as well as in non-equilibrium processes, and thereby allow to tune these properties separately for reaction steering.

Acknowledgements

We acknowledge financial support by European Research Council (ERC) Advanced Grant 695437 THz-Calorimetry. This study is funded by the Deutsche Forschungsgemeinschaft (DFG, German Research Foundation) under Germany's Excellence Strategy-EXC2033-390677874-RESOLV. We thank the Mercator Research Center Ruhr (MERCUR) for funding. This project has received funding from the European Union's Horizon 2020 programme (FP-RESOMUS - MSCA 801459). This work is supported by the "Center for Solvation Science ZEMOS" funded by the German Federal Ministry of Education and Research BMBF and by the Ministry of Culture and Research of Nord Rhine-Westphalia MKW NRW. We want to thank M. Heyden and M.-P. Gaigeot for interesting discussions. Open Access funding enabled and organized by Projekt DEAL.

Conflict of Interest

The authors declare no conflict of interest.

Data Availability Statement

The data that support the findings of this study are available from the corresponding authors upon reasonable request.

Keywords: Alcohol Hydration · Entropy · Enthalpy · Hydrophobic Hydration · THz-Calorimetry · THz Spectroscopy

[1] D. M. Huang, D. Chandler, *Proc. Natl. Acad. Sci. USA* **2000**, *97*, 8324.
[2] D. Chandler, *Nature* **2005**, *437*, 640.
[3] M. Liu, A. K. Das, J. Lincoff, S. Sasmal, S. Y. Cheng, R. M. Vernon, J. D. Forman-Kay, T. Head-Gordon, *Int. J. Mol. Sci.* **2021**, *22*, 3420.
[4] J. Wereszczynski, J. A. McCammon, *Q. Rev. Biophys.* **2012**, *45*, 1.
[5] J. M. Fox, M. Zhao, M. J. Fink, K. Kang, G. M. Whitesides, *Annu. Rev. Biophys.* **2018**, *47*, 223.
[6] M. Maurer, C. Oostenbrink, *J. Mol. Recognit.* **2019**, *32*, e2810.
[7] A. Majumdar, P. Dogra, S. Maity, S. Mukhopadhyay, *J. Phys. Chem. Lett.* **2019**, *10*, 3929.
[8] J. Ahlers, E. M. Adams, V. Bader, S. Pezzotti, K. F. Winklhofer, J. Tatzelt, M. Havenith, *Biophys. J.* **2021**, *120*, 1266.
[9] A. Ianiro, H. Wu, M. M. van Rijt, M. P. Vena, A. D. Keizer, A. C. C. Esteves, R. Tuinier, H. Friedrich, N. A. Sommerdijk, J. P. Patterson, *Nat. Chem.* **2019**, *11*, 320.
[10] W.-L. Li, T. Head-Gordon, *ACS Cent. Sci.* **2021**, *7*, 72.
[11] F. Sebastiani, T. A. Bender, S. Pezzotti, W.-L. Li, G. Schwaab, R. G. Bergman, K. N. Raymond, F. D. Toste, T. Head-Gordon, M. Havenith, *Proc. Natl. Acad. Sci. USA* **2020**, *117*, 32954.
[12] C. J. Hastings, M. D. Pluth, R. G. Bergman, K. N. Raymond, *J. Am. Chem. Soc.* **2010**, *132*, 6938.
[13] G. Marcandalli, A. Goyal, M. T. M. Koper, *ACS Catal.* **2021**, *11*, 4936.
[14] A. Serva, M. Salanne, M. Havenith, S. Pezzotti, *Proc. Natl. Acad. Sci. USA* **2021**, *118*, e2023867118.
[15] P. Clabaut, B. Schweitzer, A. W. Götz, C. Michel, S. N. Steinmann, *J. Chem. Theory Comput.* **2020**, *16*, 6539.
[16] J. Monroe, M. Barry, A. DeStefano, P. A. Gokturk, S. Jiao, D. Robinson-Brown, T. Webber, E. J. Crumlin, S. Han, M. S. Shell, *Annu. Rev. Chem. Biomol. Eng.* **2020**, *11*, 523.
[17] A. J. Patel, P. Varilly, D. Chandler, *J. Phys. Chem. B* **2010**, *114*, 1632.
[18] N. B. Rego, E. Xi, A. J. Patel, *Proc. Natl. Acad. Sci. USA* **2021**, *118*, e2018234118.
[19] E. M. Adams, S. Pezzotti, J. Ahlers, M. Rüttermann, M. Levin, A. Goldenzweig, Y. Peleg, S. J. Fleishman, I. Sagi, M. Havenith, *JACS Au* **2021**, *1*, 1076.
[20] A. Serva, M. Havenith, S. Pezzotti, *J. Chem. Phys.* **2021**, *155*, 204706.
[21] E. Duboué-Dijon, D. Laage, *J. Phys. Chem. B* **2015**, *119*, 8406.
[22] N. Galamba, *J. Mol. Liq.* **2021**, *339*, 116699.
[23] N. Giovambattista, P. J. Rossky, P. G. Debenedetti, *J. Phys. Chem. B* **2009**, *113*, 13723.
[24] N. Giovambattista, P. G. Debenedetti, P. J. Rossky, *J. Phys. Chem. C* **2007**, *111*, 1323.
[25] J. G. Davis, K. P. Gierszal, P. Wang, D. Ben-Amotz, *Nature* **2012**, *491*, 582.
[26] S. N. Jamadagni, R. Godawat, S. Garde, *Annu. Rev. Chem. Biomol. Eng.* **2011**, *2*, 147.
[27] V. Conti Nibali, S. Pezzotti, F. Sebastiani, D. R. Galimberti, G. Schwaab, M. Heyden, M.-P. Gaigeot, M. Havenith, *J. Phys. Chem. Lett.* **2020**, *11*, 4809.
[28] N. Abidi, K. R. G. Lim, Z. W. Seh, S. N. Steinmann, *WIREs Comput. Mol. Sci.* **2021**, *11*, e1499.
[29] S. E. Sanders, P. B. Petersen, *J. Chem. Phys.* **2019**, *150*, 204708.
[30] Y. Yang, F. C. Lightstone, S. E. Wong, *Expert Opin. Drug Discovery* **2013**, *8*, 277.
[31] F. Böhm, G. Schwaab, M. Havenith, *Angew. Chem. Int. Ed.* **2017**, *56*, 9981; *Angew. Chem.* **2017**, *129*, 10113.
[32] D. Chandler, P. Varilly, *Proceedings of the International School of Physics "Enrico Fermi"* **2012**, *176*, 75.
[33] K. Lum, D. Chandler, J. D. Weeks, *J. Phys. Chem. B* **1999**, *103*, 4570.
[34] S. Funke, F. Sebastiani, G. Schwaab, M. Havenith, *J. Chem. Phys.* **2019**, *150*, 224505.
[35] D. Ben-Amotz, *J. Am. Chem. Soc.* **2019**, *141*, 10569.
[36] A. J. Bredt, D. Ben-Amotz, *Phys. Chem. Chem. Phys.* **2020**, *22*, 11724.
[37] C. Weeraratna, C. Amarasinghe, W. Lu, M. Ahmed, *J. Phys. Chem. Lett.* **2021**, *12*, 5503.
[38] S. Pezzotti, A. Serva, F. Sebastiani, F. S. Brigiano, D. R. Galimberti, L. Potier, S. Alfarano, G. Schwaab, M. Havenith, M.-P. Gaigeot, *J. Phys. Chem. Lett.* **2021**, *12*, 3827.
[39] R. A. X. Persson, V. Pattni, A. Singh, S. M. Kast, M. Heyden, *J. Chem. Theory Comput.* **2017**, *13*, 4467.
[40] D. Laage, J. T. Hynes, *Science* **2006**, *311*, 832.
[41] A. A. Bakulin, M. S. Pshenichnikov, H. J. Bakker, C. Petersen, *J. Phys. Chem. A* **2011**, *115*, 1821.
[42] D. Laage, G. Stirnemann, J. T. Hynes, *J. Phys. Chem. B* **2009**, *113*, 2428.
[43] P. Schienbein, G. Schwaab, H. Forbert, M. Havenith, D. Marx, *J. Phys. Chem. Lett.* **2017**, *8*, 2373.
[44] F. Sebastiani, C. Y. Ma, S. Funke, A. Bäumer, D. Decka, C. Hoberg, A. Esser, H. Forbert, G. Schwaab, D. Marx, et al., *Angew. Chem. Int. Ed.* **2021**, *60*, 3768; *Angew. Chem.* **2021**, *133*, 3812.
[45] C. Y. Ma, S. Pezzotti, G. Schwaab, M. Gebala, D. Herschlag, M. Havenith, *Phys. Chem. Chem. Phys.* **2021**, *23*, 23203.
[46] E. Gallicchio, M. Kubo, R. M. Levy, *J. Phys. Chem. B* **2000**, *104*, 6271.
[47] J. I. Monroe, M. S. Shell, *Proc. Natl. Acad. Sci. USA* **2018**, *115*, 8093.
[48] E. Xi, V. Venkateshwaran, L. Li, N. Rego, A. Patel, S. Garde, *Proc. Natl. Acad. Sci. USA* **2017**, *114*, 201700092.
[49] V. Hande, S. Chakrabarty, *ACS Omega* **2022**, *7*, 2671.
[50] M. K. Coe, R. Evans, N. B. Wilding, *Phys. Rev. Lett.* **2022**, *128*, 045501.

Manuscript received: March 15, 2022
Accepted manuscript online: May 2, 2022
Version of record online: June 1, 2022